Coupling between external and internal mass transfer during drying of a porous medium

Andreas G. Yiotis,[1] Ioannis N. Tsimpanogiannis,[2] Athanassios K. Stubos,[1] and Yannis C. Yortsos[3]

Received 25 September 2006; revised 29 March 2007; accepted 4 April 2007; published 7 June 2007.

[1] We present a pore-network model for drying processes in porous media that couples convective-diffusive mass transfer over the external surface of a porous medium with mass transport mechanisms within the porous material, namely, the flow through liquid films that form at the pore walls and diffusion of the liquid vapors through the dry pores. We study the effects of the external boundary layer thickness, a film-based capillary number, and the Peclet number of the purge gas that flows over the porous medium surface on the shape of the drying curves and the overall recovery times. We show that the drying rate remains practically constant, as long as the liquid films span across the entire pore network and provide hydraulic connectivity between the bulk liquid front and the product surface. This condition is satisfied when the drying process is controlled by the external mass transfer over the porous medium surface, rather than mass transport (through films and diffusion) within the porous material, e.g., for large values of the boundary layer thickness and small values of the film-based capillary number. Our results explain previously reported experimental findings and provide a rigorous explanation of the experimentally reported constant-rate period.

Citation: Yiotis, A. G., I. N. Tsimpanogiannis, A. K. Stubos, and Y. C. Yortsos (2007), Coupling between external and internal mass transfer during drying of a porous medium, *Water Resour. Res.*, *43*, W06403, doi:10.1029/2006WR005558.

1. Introduction

[2] Drying of porous media is a process of significant scientific and applied interest. It involves several mechanisms emerging at the pore scale that affect the macroscopic behavior of the process. These include phase change at the liquid-gas interface, mass and heat transfer by diffusion and convection, capillarity-induced flow through wetting liquid films, and the receding of the liquid-gas interfaces under combined viscous, capillary, and buoyancy forces.

[3] In early works, the drying of porous media was approached from a phenomenological point of view, where the medium was treated as a hypothetical effective continuum, partial differential equations were used to describe the temporal and spatial evolution of volume-averaged quantities, such as temperature and moisture content, and fluxes were related to gradients through empirical coefficients. Such approaches ignored the detailed physics at the pore level and provided limited information on how the macroscopic behavior of the process is related to phenomena occurring at the pore scale.

[4] A significant improvement in modeling has been achieved in recent years through the use of pore networks to model the complicated geometries of real porous materials. Starting with the pioneering work of *Fatt* [1956], pore-network models have been used widely to study two-phase or multiphase displacement in porous media [*Blunt et al.*, 2002]. In the past 10 years, these have been extended to phase-change processes in porous media, including boiling [*Satik and Yortsos*, 1996] and solution-gas drive [*Li and Yortsos*, 1995; *Dominguez et al.*, 2000]. These models have offered insight on the physics involved and how the mechanisms occurring at the pore scale influence processes at the larger scale. Drying is a special case of phase-change and has also been studied at the pore-network level [see *Nowicki et al.*, 1992; *Prat*, 1993, 1995, 2007; *Laurindo and Prat*, 1996, 1998; *Prat and Bouleux*, 1999; *Huinink et al.*, 2002; *Yiotis et al.*, 2001, 2003, 2004, 2006].

[5] In typical drying experiments, it has been observed that at the early stages of the process the recovery rate remains practically constant. This period is known as the constant-rate period (CRP) and has been attributed to an excess of liquid at the surface pores of the porous material [*van Brakel*, 1980; *Chen and Pei*, 1989]. The CRP is followed by the falling rate period (FRP), during which the recovery rate decreases rapidly. For obvious reasons, a primary objective in the industrial drying of porous material is the prolonging of the CRP, the understanding of which has been a key goal of previous studies.

[6] With two exceptions, all the above mentioned pore-network level studies of drying focused on the mass transport mechanisms taking place within the porous medium. Mass transfer over the porous medium surface was neglected. *Laurindo and Prat* [1998] considered the presence of a diffusive mass boundary layer over the external

[1] National Center for Scientific Research "Demokritos," Aghia Paraskevi, Greece.
[2] Earth and Environmental Sciences Division, Los Alamos National Laboratory, Los Alamos, New Mexico, USA.
[3] Department of Chemical Engineering, University of Southern California, Los Angeles, California, USA.

0043-1397/07/2006WR005558$09.00

surface of the porous medium to estimate the drying rates in two-dimensional pore networks. However, they did not comment on the effect of this boundary layer on the extent of the CRP. More recently, *Prat* [2007] explored the effect of pore shape and contact angles on the drying rates in the presence of a mass boundary layer over the product surface. He concluded that the thickness of the mass boundary layer has a significant effect when the film tips reach the product surface and that the CRP ends when the films begin to recede into the porous medium. On the other extreme, *Suzuki and Maeda* [1968] focused exclusively on the external mass transfer and neglected completely the mass transfer within the porous medium. By solving the steady state convection-diffusion problem over a discontinuous source of liquid, they showed that a CRP is clearly apparent when the surface is sufficiently wet and the thickness of the mass boundary layer is much larger than the distance between the wet clusters at the product surface. In a previous study [*Yiotis et al.*, 2006] we used their interpretation to show that the CRP lasts as long as the product surface remains sufficiently wet through the continuous bulk liquid phase. The critical saturation that marks the transition to the FRP was then related to the thickness of the mass boundary layer. However, in that study we neglected the effect of liquid film transport within the porous medium, which is an important mass transport mechanism.

[7] For a complete description of the drying process, mass transfer in the boundary layer must be solved in conjunction with the complete mass transport within the porous medium because the local mass transfer coefficient at the external product surface depends on the mass transfer conditions within the boundary layer over the surface, as well as on the liquid distribution within the porous medium itself. This paper presents a coupled pore-network model to accomplish such a solution. The model accounts for mass transfer by diffusion and flow through liquid films within the porous medium, and convective-diffusive mass transfer through the boundary layer over the surface. For simplicity, we focus on drying at sufficiently large distances from the gas inlet, so that the thickness of the boundary layer can be considered constant in the domain of the numerical investigation.

[8] We analyze the effects of the external boundary layer thickness, a film-based capillary number, and the Peclet number of the purge gas that flows over the porous medium surface on the shape of the drying curves and the overall recovery times. Our results show that the drying rate remains practically constant, as long as the liquid films span across the entire pore network and provide hydraulic connectivity between the bulk liquid front and the product surface. This condition is satisfied when the drying process is controlled by mass transfer over the porous medium surface, rather than mass transport through films and diffusion within the porous material, namely, for large values of the boundary layer thickness and small values of the film-based capillary number. As the bulk liquid interface recedes deeper in the pore space, the liquid films at the product surface become thinner and the surface liquid saturation decreases. When the films become thin enough, they cannot sustain a liquid flux at the same rate as the rate that liquid vapors are transferred by diffusion and convection through the mass boundary layer. From that point on the drying process is controlled by the mass transfer inside the porous medium, e.g., through capillarity-induced flow through the liquid films rather than mass transfer through the mass boundary layer. The drying rate is decreasing during this period as the surface films become thinner. Our results explain previously reported experimental findings and provide a rigorous explanation of the constant-rate period.

[9] The paper is organized as follows: First, we provide the problem formulation. This includes a brief review of preliminary material, a statement of the problem, an analysis of the simpler one-dimensional (1-D) geometry, which gives useful insights, and the full solution of the 3-D problem using a pore-network model. Then, the results are compared with the 1-D analysis, and subsequently with those of *Suzuki and Maeda* [1968]. We focus on effects of the external boundary layer thickness, the capillary number, both of which are found to be key parameters, and on the effect of the Peclet number, which under the assumption of a constant boundary layer thickness, far downstream of the drying process, is found to be weak. Of course, the Peclet number does affect the process significantly, but indirectly, through its effect on the boundary layer thickness.

2. Problem Formulation

[10] We consider the isothermal drying of a porous medium saturated with a volatile single-component liquid, as shown in Figure 1. The schematic represents a unit cell of the drying process in the porous medium. All sides, except one, denoted in the figure as surface S, are either impermeable or periodic to fluid flow and mass transfer. Surface S is exposed to a gas which is flowing parallel to it with characteristic velocity U_∞, purging the vapor by convection and diffusion. A mass transfer layer of thickness δ_m develops, at the outer side of which the vapor pressure of the volatile component is zero. We recall that for boundary layer flow over a flat plate and a fixed surface concentration, δ_m is well approximated by the expression [e.g., *Bird et al.*, 1960; *Leal*, 1992]

$$\delta_m = \delta \mathrm{Sc}^{-1/3}. \tag{1}$$

Here δ is the momentum boundary layer thickness, $\mathrm{Sc} = \nu/D_e$ is the Schmidt number, ν is the gas kinematic viscosity, D_e the gas phase diffusivity, and we have

$$\delta \approx 4.64X\ \mathrm{Re}_X^{-1/2}, \tag{2}$$

where $\mathrm{Re}_X = U_\infty X/\nu$ is the local Reynolds number (at the downstream location X) and U_∞ is the free-stream gas velocity. In the drying of a porous medium, the boundary layer will also be affected by the two additional factors: that surface S is permeable, and its surface concentration nonuniform and variable. While interesting and potentially important, uncovering this dependence is not the purpose of this paper, whose focus is to understand the effects of external mass transfer on the drying process, given a boundary layer thickness. As mentioned, this study is valid at the periodic mass boundary regime, when the thickness of the boundary layer is constant, namely, at sufficiently large distances from the purge gas inlet. Extending (1) and (2) to boundary layer flow over a drying porous medium is certainly a subject worth exploring in the future.

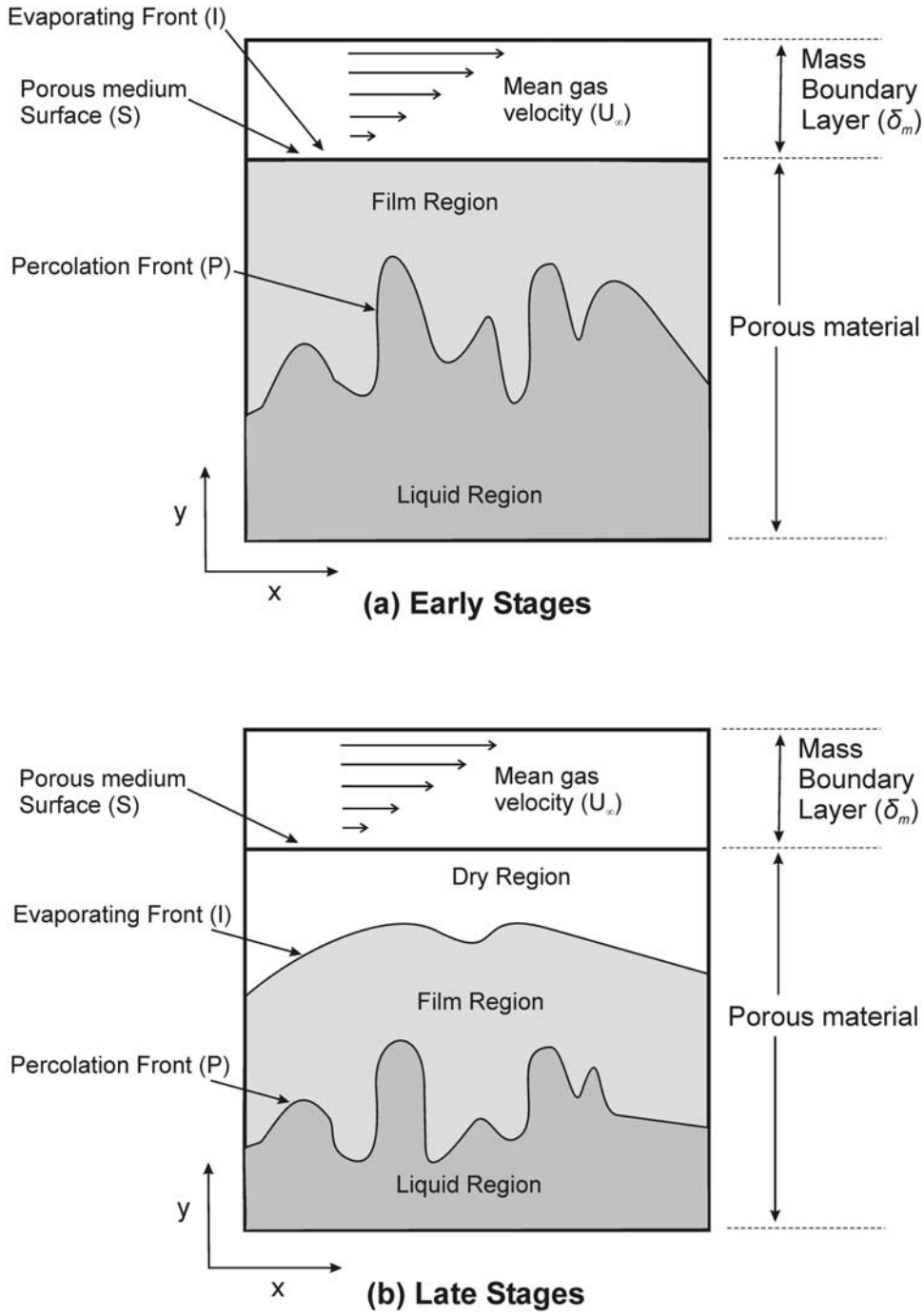

Figure 1. Schematic of the geometry considered for the drying of a porous medium. A unit cell, assumed representative of conditions at a sufficiently downstream location, is shown. (a) Early stages of the process, when liquid films reach the external surface S. (b) Late stages, when liquid films do not reach the surface. Volatile liquid evaporates and is transported by diffusion or through liquid films to S where it is purged by a gas, flowing parallel to it. The mass transfer boundary layer has thickness δ_m. Periodic boundary conditions apply on the lateral sides of the porous medium. The bulk liquid recedes following invasion percolation rules.

[11] When decoupled from external mass transfer, the drying of a porous medium has been extensively analyzed. At any given time, one identifies three distinct regions (Figure 1): a bulk-liquid region, consisting of the volatile liquid; a film region, where liquid films coexist with saturated gas; and a dry region, consisting of only the unsaturated gas phase. By a combination of film flow and diffusion, the volatile species is transferred to surface S, where it is purged. In general, the bulk liquid-gas interface (denoted by P in Figure 1) obeys invasion percolation rules,

namely, as the volatile species vaporizes, it recedes by vacating the largest perimeter throat it occupies at the given time. In this drainage process, films are left in the corners of the pores, through which liquid can flow by capillary action to the evaporation front (denoted by I in Figure 1b). As noted, the latter can be located at the surface S, within the porous medium, or partly at the surface S and partly within the porous medium, depending on whether or not films terminate at S (depicted in Figure 1 as early or late stages, respectively). When the films terminate inside the porous medium, the liquid evaporates at the film tips (evaporation front I) and is transported to S by gas phase diffusion.

[12] In previous studies [*Yiotis et al.*, 2003, 2004] we showed that inside the porous medium and under quasi-static conditions, the process in either the film region or in the unsaturated gas can be described by the Laplace equation. This is because both in viscous flow in the films and in diffusion in the gas phase, the mass flux is linearly proportional to the driving force (pressure or concentration gradients, respectively). Then, the combined problem can be solved by defining an extended variable $\Phi = (\rho^3 + \zeta Ca_F)/(1 + Ca_F)$, where ρ is the normalized thickness of the films (equal to 1 at the percolation front), ζ is the normalized gas phase concentration of the volatile species (equal to 1 in the entire film region), and Ca_F is a (modified) film-based capillary number, defined as $Ca_F = \pi D C_e \mu_l / 2\alpha r_0 \rho_l \gamma$. Here γ is the interfacial tension, D is the diffusion coefficient of the liquid vapors, C_e is the equilibrium concentration, μ_l is the liquid viscosity, ρ_l is the liquid density, r_0 is the characteristic pore size, and α is a constant that depends on the shape of the pore cross section. Through the above substitution, we have shown [*Yiotis et al.*, 2003] that variable Φ satisfies the Laplace equation in the domain outside the percolation front and inside the porous medium (i.e., in the region bounded by surfaces P and S in Figure 1):

$$\nabla^2 \Phi = 0 \ . \tag{3}$$

One can then determine the position of the film tips, and hence of the evaporation front I, by the surface which satisfies $\Phi_I = Ca_F/(1 + Ca_F)$.

[13] When mass transfer through the external layer is infinitely fast (for example, in the absence of mass boundary layer over the external surface of the porous medium), surface S is completely dry ($\rho = \zeta = 0$) and the problem reduces to solving (3) subject to boundary conditions $\Phi = 1$ at the percolation front and $\Phi = 0$ at S. The calculations of drying rates, the film thickness profiles, and other quantities relevant to drying follow in a straightforward manner and were in detail discussed by *Yiotis et al.* [2003, 2004]. In this case the drying process is controlled by viscous flow through the films and the dimensionless drying rate $\Im_{D,\infty}$ (defined as $\Im_{D,\infty} = -\int_S (\partial\Phi/\partial n) dS$) is independent of Ca_F. In particular, the plot of the dimensionless flux $\Im_{D,\infty}$ versus the dimensionless time τ, defined as

$$\tau = t \Big/ \left(\left(\frac{16a}{\pi^2} \right) \left(\frac{V_p \rho_L}{r_c D_e C_e} \right) \left(\frac{Ca_F}{1 + Ca_F} \right) \right),$$

depends only on the geometry of the porous medium and is independent of the capillary number Ca_F, for all capillary numbers less than of the order of 0.01. Of course, the dimensional drying rate is a function of Ca_F through

$$F \propto -\frac{D_e C_e}{Ca_F} (1 + Ca_F) \Im_D \tag{4}$$

[*Yiotis et al.*, 2004]. In the above, we have used subscript ∞ to denote this particular solution and defined V_p as the typical pore volume, r_c the throat diameter, C_e the equilibrium concentration of the liquid vapors, ρ_L the liquid phase density, and α a geometric parameter that depends on the shape of the throats [*Ransohoff and Radke*, 1988; *Dong and Chatzis*, 1995]. The variation of $\Im_{D,\infty}$ with the liquid saturation inside the porous medium, S_L, which is also practically independent of the capillary number for typical conditions, will be compared later with the case when external mass transfer is not negligible.

[14] In the general case, the external mass transfer is not infinitely fast, a dry interface cannot be maintained on the external boundary S, and the above solution is not valid. In fact, the external mass transfer cannot be decoupled from the porous medium process and a new approach is needed. This necessary coupling is the main and novel issue addressed in the paper.

3. Coupling of the External Mass Transfer With Drying in the Porous Medium

[15] External mass transfer proceeds by advection along the x-direction and by diffusion along the x- and y-directions (Figure 1). Under quasi-static conditions, the conservation of mass in dimensionless notation reads

$$u \frac{\partial \Phi}{\partial x} = \frac{1}{Pe} \nabla^2 \Phi \quad \text{in} \quad 0 < x < n, \ 0 < y < d, \tag{5}$$

where we introduced the dimensionless velocity $u = U/U_\infty$, the spatial coordinates were scaled with a characteristic pore length scale l, and we defined the rescaled mass boundary layer thickness $d = \delta_m/l$ and the pore-scale Peclet number, $Pe = U_\infty l/D_e$. Equation (5) is subject to a dry condition at the edge of the boundary layer, $\Phi(x, y = d) = 0$ and to periodic boundary conditions at $x = 0$ and $x = n$. In the latter, we implicitly assumed a unit cell sufficiently downstream.

[16] Inside the porous medium, $P(x, t) < y < 0$ (where we defined the location of the percolation front, $y = P(x, t)$), the mechanisms discussed by *Yiotis et al.* [2004] remain valid, namely, viscous flow in the films, diffusion in the gas phase, and the receding of the bulk liquid interface following percolation rules. (Gas phase convection within the porous medium may be important, but only at large Peclet numbers [*Yiotis et al.*, 2001], and will be ignored). Hence the Laplace equation (3) remains applicable:

$$\nabla^2 \Phi = 0 \qquad \text{in} \qquad 0 < x < n, \ P(x,t) < y < 0. \tag{6}$$

The boundary conditions for the solution of (6) depend on the existence of films at the surface S, as follows:

[17] 1. When there are no bulk liquid interfaces or film menisci on S, then continuity of Φ and its normal flux apply (note that the effective diffusion coefficients are different in

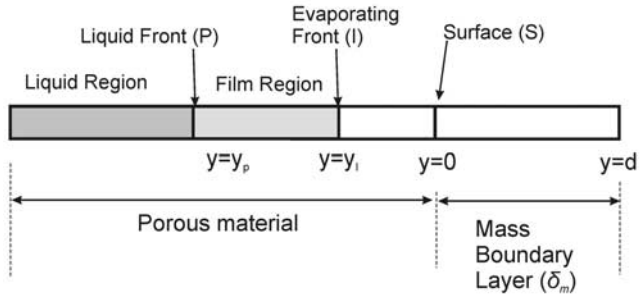

Figure 2. Schematic of the drying problem in one-dimensional (1-D) geometries, when the films do not reach up to the surface S of the porous material (case 1 in the text).

the two domains). For example, this will be the case at the later stages of drying (Figure 1b).

[18] 2. When a bulk liquid or a film interface exists at any point on S (e.g., Figure 1a), the quantity Φ becomes discontinuous at those points: Right outside the porous medium there is no liquid film ($\rho = 0$), the gas phase is saturated ($\zeta = 1$), and $\Phi = Ca_F/(1 + Ca_F)$; while right inside the porous medium, the film has a finite thickness ρ^*, and the gas phase remains saturated, thus leading to a discontinuity in Φ. Indeed, we can show that requiring continuity for all films or liquid interfaces on S (a condition which remains fully valid when the films terminate inside the porous medium as in case 1), renders the problem over-specified. We will demonstrate this shortly by considering the simple case of 1-D geometry. Before proceeding, we remark that in this case and in reality, the film thickness will decrease rapidly near S (within a single pore perhaps) and vanish at the surface S. However, in the context of this work as well as of the previous works, where the pore space is discretized in terms of distinct pores coupled through discrete bonds, this detail cannot be captured, and hence we must assume a nonzero value $\rho^* > 0$, which is an effective thickness average, at the surface S.

3.1. One-Dimensional Geometry

[19] To obtain some insight on the more complex 3-D problem, we first consider the simpler 1-D geometry. In this case, mass transfer in the external layer ($0 < y < d$) is by diffusion only, and equation (5) is replaced by steady state diffusion in the y-direction. Take the bulk liquid at location $y = y_P < 0$, the surface S at $y = 0$, and the edge of the boundary layer at $y = d$ (Figure 2). We can distinguish two different cases:

[20] In case 1, the films terminate inside the porous medium and the two problems are coupled by continuity in Φ and its flux at $y = 0$ (Figure 2). The solution of the problem can be found readily,

$$\Phi_i = \frac{(d-y)}{d-\lambda y_p} \qquad \text{in} \quad 0 < y < d \tag{7}$$

and

$$\Phi_i = 1 + \frac{\lambda(y_P - y)}{d - \lambda y_P} \qquad \text{in} \qquad y_P < y < 0, \tag{8}$$

where $\lambda > 1$ is the ratio of diffusivities (external to internal, and include also the porosity of the porous medium). In particular, the dimensionless flux

$$-\left.\frac{\partial \Phi_i}{\partial y}\right|_{0-} = \frac{\lambda}{d - \lambda y_P} \tag{9}$$

varies with the process (through y_P) and decreases as the thickness of the external mass transfer layer increases (Figure 3). Clearly, for self-consistency of this case, the location $y = y_I$, where $\Phi = Ca_F/(1 + Ca_F)$ and the films terminate, must lie inside the porous medium ($y_I \geq 0$), as films cannot exist outside the porous medium, namely, $\Phi_I = [Ca_F/(1 + Ca_F)] \leq \Phi_i(0^-)$. Using (8), this constraint can be shown to be

$$\frac{d}{\lambda} \leq -Ca_F y_P. \tag{10}$$

If this condition is violated (an event that will happen early in the process), then we must revisit the problem and impose a discontinuity in Φ at $y = 0$, as we remarked above.

[21] In case 2, the films terminate at the surface S, at which point function Φ becomes discontinuous, the film thickness being equal to ρ^* on the porous medium side and zero on the external side. Then,

$$\Phi_{ii}(0-) = \frac{\rho^{*3} + Ca_F}{1 + Ca_F}, \Phi_{ii}(0+) = \frac{Ca_F}{1 + Ca_F},$$
$$\Phi_{ii}|_-^+ = -\frac{\rho^{*3}}{1 + Ca_F}. \tag{11}$$

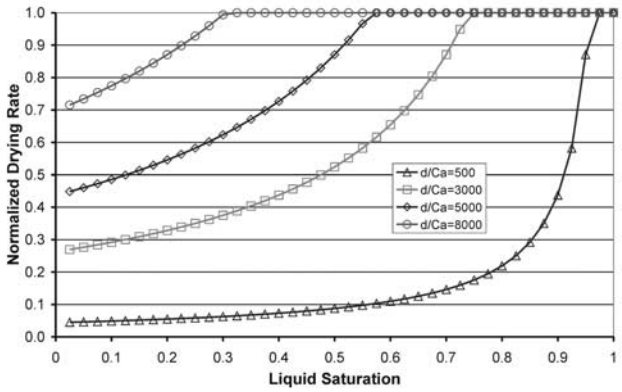

Figure 3. The variation of the normalized drying rate for the 1-D problem, as a function of the liquid saturation. The dimensionless drying rates $\Im_D$ were normalized with the flux from equation (15). At the early stages of the process, the films reach the external surface and the dimensionless rate is constant, given by (15). At a critical saturation given by equation (17), the films are not sufficiently long to reach the outer surface and the rate decreases with the liquid saturation, as given by equation (9). The critical saturation decreases with an increase in the external mass transfer layer thickness and with a decrease in the capillary number. $Ca_F = 0.01$, $\lambda = 230$, $n = 50$.

As before, we can calculate Φ analytically

$$\Phi_{ii} = \frac{(d-y)}{d}\frac{Ca_F}{(1+Ca_F)} \quad \text{in} \quad 0 < y < d \tag{12}$$

and

$$\Phi_{ii} = 1 + \frac{(y_P - y)}{y_P}\frac{(\rho^{*3}-1)}{(1+Ca_F)} \quad \text{in} \quad y_P < y < 0. \tag{13}$$

Continuity of flux at y = 0, $(\partial\Phi_{ii}/\partial y)|_- = \lambda(\partial\Phi_{ii}/\partial y)|_+$ gives

$$\rho^{*3} = 1 + \frac{\lambda Ca_F y_P}{d}. \tag{14}$$

Now the dimensionless flux

$$-\left.\frac{\partial\Phi_{ii}}{\partial y}\right|_{0-} = -\frac{\lambda Ca_F}{d(1+Ca_F)} \tag{15}$$

remains constant throughout the process, decreasing as the thickness of the external mass transfer layer increases or as the capillary number decreases (Figure 3). Self-consistency with the assumption made requires $0 < \rho^* < 1$, which can be shown to be satisfied when

$$\frac{d}{\lambda} > -Ca_F y_P, \tag{16}$$

thus complementing condition (10). As long as (16) is in effect (e.g., early in the process), films terminate at the surface but with a nonzero thickness ρ^* on the porous medium side of the surface S. The thickness of the films at the surface decreases with time. The film termination condition $\rho^* = 0$ is reached when $y_P = -(d/\lambda Ca_F)$, corresponding to $\Phi(0) = Ca_F/(1 + Ca_F)$ and a continuous Φ at that point, as expected.

[22] The variation of the dimensionless flux with the saturation, given here by the relation $S = 1 + (y_P/n)$, where n is the domain size, is shown in Figure 3 for different values of the ratio d/Ca_F. At the early stages of the process, the films reach the external surface and the dimensionless rate is constant, following equation (15). At a critical saturation given by the equality sign in (16),

$$S^* = 1 - \frac{d}{\lambda Ca_F n}, \tag{17}$$

films are not sufficiently long to reach the outer surface and the dimensionless rate decreases with the liquid saturation following equation (9). The critical saturation decreases, and hence the constant-rate period increases, as the relative size of the external layer increases and/or as the capillary number decreases according to the ratio d/Ca_F. Note that this dependence is inverse to that for the constant rate (equation (15)).

[23] The 1-D analysis above reveals an important result, that when external mass transfer is the limiting step, the drying rate is constant. This is due to the films reaching all the way to the external surface and supplying the flux required by the external mass transfer. Clearly, this will be the case at the beginning of the process. However, at later stages, the rate is dictated by the drying process inside the porous medium in combination with the external mass transfer and decreases as the process goes on. In 1-D the transition point was found to be an increasing function of the ratio of the boundary layer thickness to the capillary number. We anticipate qualitatively similar results for the full 3-D problem, which is discussed below. We noted earlier that the "wetness" of the surface S (but explained without the consideration of films) has been advanced as a reason for the constant rate period by *Suzuki and Maeda* [1968] and *van Brakel* [1980]. A comparison with their results will be given in a later section.

3.2. Three-Dimensional Geometries

[24] To proceed with the more complex 3-D geometries, we follow closely the 1-D approach. At the onset of drying, all pore throats at S are occupied by bulk liquid interfaces. During this stage, the drying rates are computed by solving the external mass transfer problem (5) using saturated-gas boundary condition at S, $\Phi(x, y = 0) = 1$, and a dry-gas condition at the edge of the boundary layer, $\Phi(x, y = d) = 0$. As drying proceeds, bulk-liquid interfaces will recede, creating liquid films at various surface pores (denoted above as case 2). At any given time step, a surface pore containing a bulk-liquid interface may become a film-containing pore. Simultaneously, the film thickness ρ^* on other surface pores will decrease. Because of the possibility of discontinuities in Φ at various surface points, which are not known in advance, finding the complete solution requires an iterative approach. The key is identifying the next surface pore where a bulk-liquid interface will recede and film will develop (and where Φ will have a jump), and also finding the respective jumps for all other surface pores containing films. This iterative algorithm must ensure the following:

[25] 1. If a surface pore does not contain liquid films, namely, the pore is completely dry, condition $\Phi < Ca_F/(1 + Ca_F)$ applies and Φ is continuous across S at that pore.

[26] 2. If a surface pore contains liquid films, then the value of Φ is discontinuous at S, with a value $\Phi > Ca_F/(1 + Ca_F)$ on the porous medium side of S and $\Phi = Ca_F/(1 + Ca_F)$ on the mass boundary layer (external) side.

[27] 3. For either case on surface S, continuity of normal fluxes applies.

[28] 4. As in previous works, the bulk-liquid interfaces recede following invasion percolation rules.

[29] We devised an efficient computational algorithm based on iterative successive over-relaxation that satisfies all these requirements and converges to the true solution. The problem is characterized by the dimensionless parameters d, Ca_F, Pe, and n, the effect of the first three of which was studied. The porous medium was represented as a cubic pore network (corresponding essentially to a finite difference model) of size $50 \times 50 \times 50$ ($n = 50$). As noted before, lengths were made dimensionless with the lattice pore spacing.

4. Results

[30] First, we considered the solution of the problem in the absence of advection, where mass transfer is purely diffusive ($Pe = 0$).

4.1. Diffusive Mass Transfer in the Boundary Layer (Pe = 0)

[31] When the liquid films reach the product surface, the dimensionless drying rate, $\Im_D = -\int_S (\partial\Phi/\partial n)dS$, is propor-

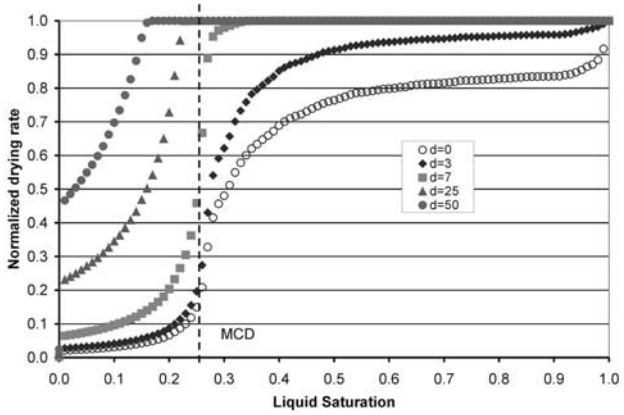

Figure 4. Normalized drying rate curves for various values of the boundary layer thickness d and for a fixed value of $Ca_F = 0.01$ in the limit when the external mass transfer is strictly diffusive ($Pe = 0$) ($50 \times 50 \times 50$ pore networks). A constant-rate period (CRP) is clearly apparent for $d = 7$, 25, and 50. For such relatively large values of Ca_F, the films remain in contact with the product surface S only when d is sufficiently large. Otherwise, it is dry. The curve corresponding to $d = 0$ is similar to that reported by *Le Bray and Prat* [1999] in the absence of films and reproduced here from *Yiotis et al.* [2003].

tional to $Ca_F/(1 + Ca_F)$ and inversely proportional to the thickness of the mass boundary layer d, following the 1-D result (equation (15)). This expression is valid for the 3-D problem as well, because at the beginning of drying the bulk liquid front is flat. Figure 4 shows plots of the dimensionless drying rate, $\Im_D$ (also normalized with respect to its maximum value at the beginning of the process given by equation (15)), versus the overall liquid saturation for various values of the film thickness d and for a fixed value of $Ca_F = 0.01$. Plotted also is the limit considered by *Yiotis et al.* [2003], denoted by $d = 0$, where the external layer has zero thickness (and external mass transfer is infinitely fast). In close analogy with the 1-D analysis, a constant rate period (CRP) emerges, the extent of which increases with increasing d. For small values of d, e.g., for $d = 3$, the films lose contact with the product surface S soon after the beginning of the process and the surface rapidly dries out. At larger values, e.g., for $d = 7$, the films remain in contact with S for a sufficiently long time leading to a sustained CRP. During this period, mass transfer through the boundary layer is the limiting mechanism and the dimensional drying rate is a function of the boundary layer thickness. Note that in Figure 4 we have chosen a relatively high capillary number, as otherwise, for the specific lattice size, the films will remain long, spanning the entire pore network throughout the process (and the drying rates remain constant practically for all values of the thickness considered). Analogous is the dependence of the plot of the dimensionless drying rate versus the overall liquid saturation for various values of the capillary number Ca_F for a constant d, as shown in Figure 5. We note the existence of a CRP the extent of which increases as the capillary number decreases, for the same reasons as explained in Figure 4.

[32] Also shown in Figures 4 and 5 is the critical saturation value, corresponding to the main cluster disconnection (MCD) point. This point was argued to represent the demarcation of the end of the CRP (in the absence of films) by *Yiotis et al.* [2006]. While a good approximation when the external mass transfer is fast (small thickness of the boundary layer), it is apparent that it fails for larger values of d, where the CPR can last for a period longer than the MCD. In fact, in the presence of films, the termination of the CRP regime is associated with the condition of films not reaching the external surface for the first time, as in the 1-D case. The end of the CRP coincides when the films start disconnecting from the surface. Therefore, for a CRP to exist, it is not necessary that bulk liquid-gas interfaces exist at the surface pores. Because drying is driven by concentration differences, the CRP would last as long as the vapor concentration at the outlet boundary remains practically constant. This is certainly the case when the surface contains films, in which case the concentration is equal to the saturation value. Because of film flow, the surface remains significantly wet even at late stages of the process, maintaining a constant driving force for drying, and hence a constant rate period.

[33] While larger thickness leads to a prolonged CRP, the corresponding effect on the dimensional rate is shown in Figure 6, where dimensional drying rates for various values of the mass boundary layer thickness d and fixed $Ca_F = 0.01$ are plotted as a function of the liquid saturation. For $d \geq 4$ the process is controlled by mass transfer through the boundary layer at early times and a constant rate period is clearly apparent (which, as noted in equation (15), is proportional to $1/d$). At later times, as the product surface dries up, drying is controlled by mass transport mechanisms within the porous medium, namely, by film flow and diffusion. The drying curves then collapse to a single characteristic curve denoted by $d = 0$. For d less than 4, the liquid films do not reach the product surface and drying is controlled by mass transport through the porous medium throughout the process and all curves collapse to the $d = 0$ curve. This curve (also the top curve in Figure 6) shows the

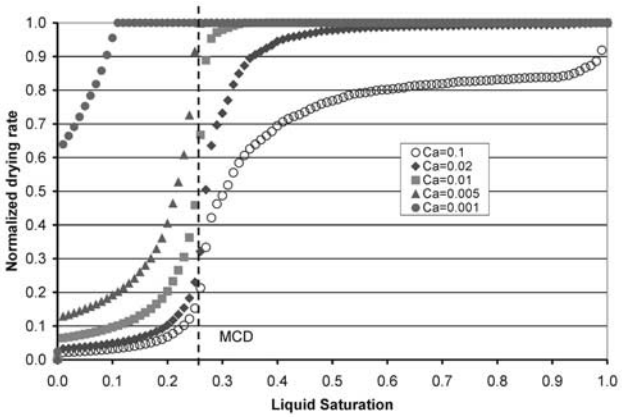

Figure 5. Normalized drying rate curves for various values of the capillary number Ca_F and for a fixed boundary layer thickness $d = 7$ in the limit when the external mass transfer is strictly diffusive ($Pe = 0$) ($50 \times 50 \times 50$ pore networks). A constant-rate period (CRP) is clearly apparent for Ca < 0.01.

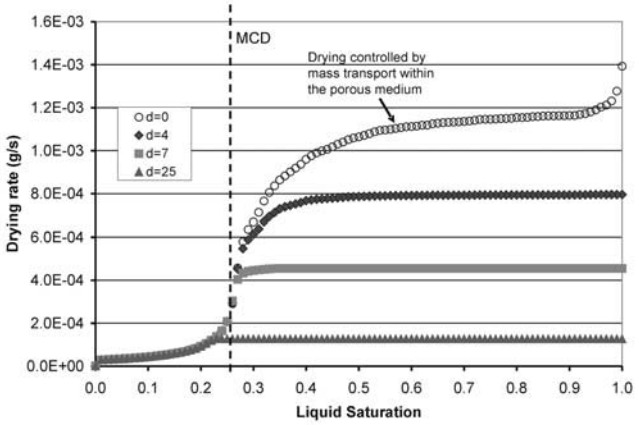

Figure 6. Dimensional drying rates for various values of the mass boundary layer thickness d and fixed $Ca_F = 0.01$. For $d \geq 4$ the process is controlled by mass transfer through the boundary layer at early times and a constant-rate period is clearly apparent. In this case the drying rate is proportional to $1/d$ (equations (4) and (15)). At later times, as the product surface dries up, drying is controlled by mass transport mechanisms within the porous medium, namely, by film flow and diffusion. The drying curves then collapse to a single characteristic curve denoted by $d = 0$. For d less than 4, the liquid films do not reach the product surface and drying is controlled by mass transport through the porous medium and all curves collapse to the $d = 0$ curve. This curve (also the top curve in the figure) shows the drying rate in the absence of a mass boundary layer [*Le Bray and Prat*, 1999; *Yiotis et al.*, 2006]. The curve marks the largest value of the drying rate with respect to the liquid saturation for a fixed value of Ca_F.

drying rate in the absence of a mass boundary layer [*Le Bray and Prat*, 1999; *Yiotis et al.*, 2006]. This curve marks the largest value of the drying rate with respect to the liquid saturation for a fixed value of Ca_F.

[34] The dependence of the critical saturation, and of the (nonnormalized) constant rate in the CRP, as a function of the ratio of the thickness to the capillary number is plotted in Figure 7. We note that the 1-D result for the rate (equation (15)), fits the 3-D data very well, as expected. By contrast, the 1-D result for the critical saturation (equation (17)) does not, reflecting the very different phenomena associated with 3-D drying. The two results, however, have a similar qualitative dependence on the ratio d/Ca_F. This is also expected. Figure 8 shows the surface film saturation (percentage of surface pores that contain films) versus the overall bulk liquid saturation for various values of the boundary layer thickness d and conditions identical to Figure 4. The product surface remains wet when the surface film saturation is high. This occurs at smaller values of the overall liquid saturation in the porous material, when the mass boundary layer thickness is larger.

[35] We summarize these findings as follows: When d is small, the rate dependence is close to that reported by *Le Bray and Prat* [1999] and recently elaborated on by *Yiotis et al.* [2006]. Because of the absence of films reaching the surface, a constant-rate period requires that a significant fraction of the surface pores be occupied by bulk liquid-gas interfaces, so that the concentration at the surface remains close to its maximum value. This mechanism is qualitatively different than when the boundary layer is thick, and where the CRP behavior emerges as a result of the existence of film-containing surface pores. This result is new and demonstrated here for the first time.

4.2. Effect of the Peclet number

[36] The effect of the Peclet number was investigated by varying its value, while keeping the mass boundary layer thickness d and the capillary number Ca_F constant. The velocity profile was taken as piston-like or linearly varying with y. Figure 9 plots the dependence of the dimensionless drying rate $\Im_D$ on saturation for different Peclet numbers and for "small" values of the ratio d/Ca_F corresponding to a short range CRP. In all cases, the effect of the Peclet number is rather weak (always for a fixed boundary layer thickness) and the results are qualitatively similar to the diffusive case. Because of the periodic conditions imposed on the lateral boundaries in the external mass transfer layer, the effect of the Peclet number (in addition to affecting the actual layer thickness, which is not considered in Figure 9) is to only affect the concentration contours. Indeed, at full saturation all curves have the same rate, which is equal to that for the purely diffusive case, equation (15). As the process

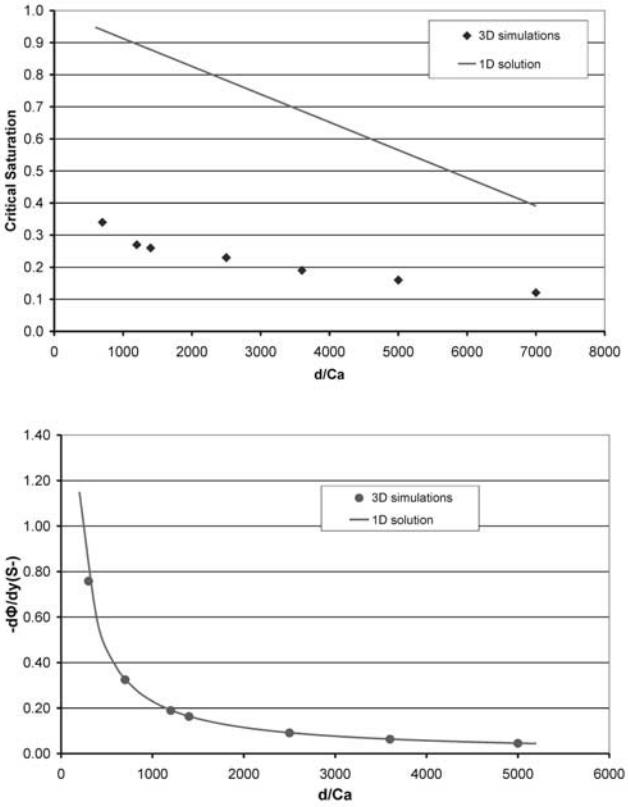

Figure 7. Plot of the critical saturation and of the dimensionless constant rate versus the ratio of the boundary layer thickness to the capillary number, d/Ca_F. Plotted also are the 1-D relations (17) and (15) for the critical saturation and the dimensionless drying rate. The MCD, often taken to indicate the end of the CRP, does not coincide with the critical saturation, highlighting the importance of films in this process. Here $0.005 \leq Ca_F \leq 0.02$, $7 \leq d \leq 50$.

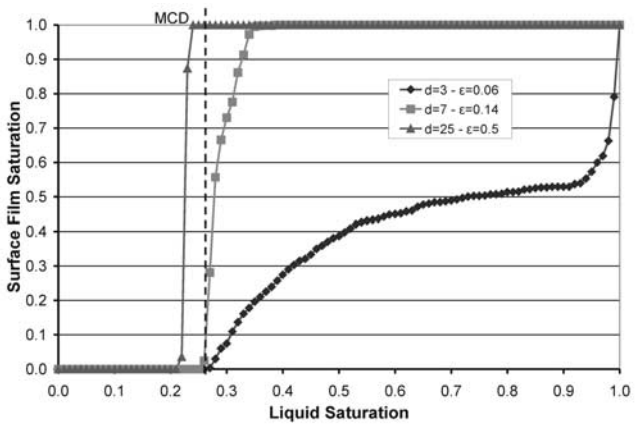

Figure 8. Surface film saturation (percentage of surface pores that contain films) versus the overall bulk liquid saturation for various values of the boundary layer thickness d (or $\varepsilon = d/n$) and fixed $Ca_F = 0.01$ ($50 \times 50 \times 50$ pore networks). The normalized drying rates under similar conditions are shown in Figure 4.

continues, higher values in the Peclet number lead to more uniform concentration profiles, with the concentration at the surface S being close to saturation, as long as there are any films on the surface. As a result, the rate is kept constant for a longer period of time, and the critical saturation decreases. The effect is the same regardless of the particular velocity profile used. At much larger values of the ratio d/Ca_F, the extent of the CRP is larger, much like in the diffusive case (Figure 10). We conclude therefore that for the fully developed case, and for a cell sufficiently downstream, the effect of the Peclet number is primarily through its effect on the boundary layer thickness d itself, and as expressed through relationship (15). We noted that the dependence of the boundary layer thickness on the Peclet number can be roughly approximated, e.g., as shown by *Bird et al.* [1960] and *Leal* [1992], although finding an accurate dependence requires further study.

4.3. Comparison With the Work of *Suzuki and Maeda* [1968]

[37] For completeness, we compare our findings with those of *Suzuki and Maeda* [1968]. The latter authors solved the concentration profile in the external mass transfer layer only, assuming periodic boundary conditions at the sides, and the following condition on the surface S:

$$\zeta = 1 \quad \text{for} \quad 0 < x < nS_{LS}, \quad \text{and} \quad \frac{\partial \zeta}{\partial y} = 0 \quad \text{for} \quad nS_{LS} < x < n. \tag{18}$$

Boundary condition (18) reflects a surface with a wet part (of fraction equal to the saturation S_{LS}) and a dry part (of fraction equal to 1-S_{LS}), which is a no-flux boundary. In the Suzuki and Maeda model, coupling between the external layers and the porous medium is approximated by the boundary condition (18), thus bypassing the need to solve the porous medium problem. In the absence of external advection, when conditions are diffusive, the Laplace equation is solved in the external layer

$$\nabla^2 \zeta = 0 \quad \text{in} \quad 0 < x < n, \quad 0 < y < d \tag{19}$$

subject to the boundary conditions in (18). To compare our results with the Suzuki and Maeda approach, we plotted the drying rates we computed in our 3-D model, as a function of the surface saturation, expressed as the percentage of

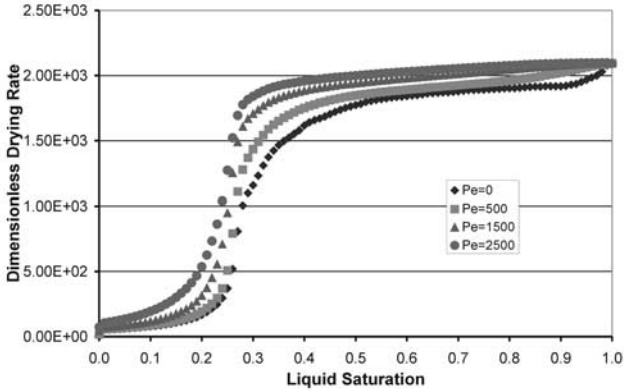

Figure 9. Dimensionless drying rate curves for various values of the Peclet number, a piston-like velocity profile, and for fixed values of the boundary layer thickness $d = 25$ and $Ca_F = 0.1$ ($50 \times 50 \times 50$ pore networks). Because of the periodic conditions imposed, the effect of the Peclet number is only through the concentration contours. Higher values of the Peclet number keep the surface at concentrations close to saturation, thus extending the CRP. The value of the rate in that regime is independent of the Peclet number and equal to that from equation (15) (multiplied by the product surface area n^2): $\Im_D = -\int_{S^-} (\partial\Phi/\partial n) dS = -n^2 [\lambda Ca_F/d(1 + Ca_F)]$.

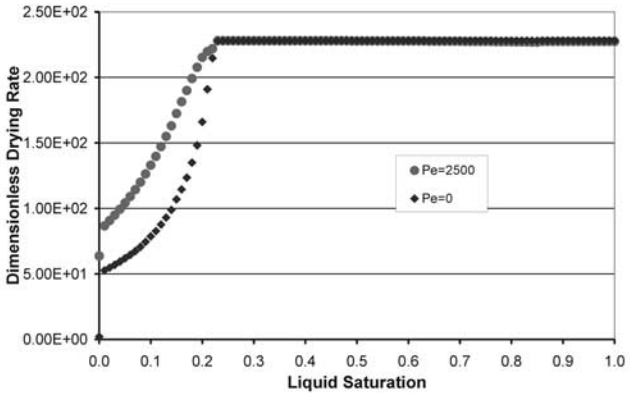

Figure 10. Dimensionless drying rate curves for various values of the Peclet number, a piston-like velocity profile, and for fixed values of the boundary layer thickness $d = 25$ and $Ca_F = 0.01$ ($50 \times 50 \times 50$ pore networks). Because of the periodic conditions imposed, the effect of the Peclet number is only through the concentration contours. Higher values of the Peclet number keep the surface at concentrations close to saturation, thus extending the CRP. The value of the rate in that regime is independent of the Peclet number and equal to that from equation (15) (multiplied by the product surface area n^2).

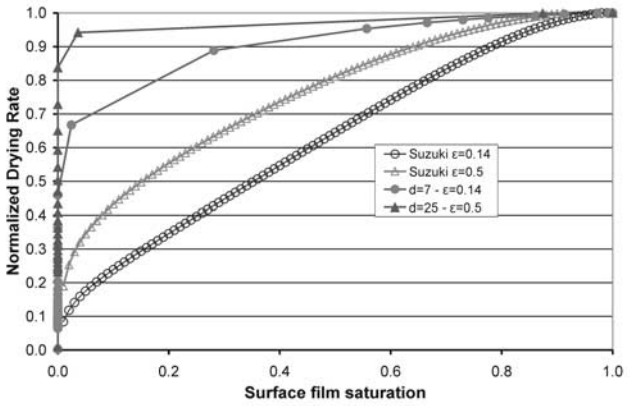

Figure 11. Normalized drying rate versus surface film saturation (percentage of surface pores that contain films) for $Ca_F = 0.01$, $d = 7$ ($\varepsilon = d/n = 0.14$), and $d = 25$ ($\varepsilon = 0.5$) in the limit when the external mass transfer is strictly diffusive ($Pe = 0$) ($50 \times 50 \times 50$ pore networks). The curves match qualitatively, although not quantitatively, the results obtained by *Suzuki and Maeda* [1968]. Lack of quantitative agreement is due to the different coupling between the porous medium and the external layer, which in the *Suzuki and Maeda* [1968] case is simplified by a no-flux condition over the nonwet region.

surface pores that contain films (Figure 11). Note that this saturation is not the same as that of the bulk.

[38] Before commenting on the comparison with the model by *Suzuki and Maeda* [1968], we note that while analytical solutions of (19) subject to (18) are possible, we will consider here results in two asymptotic limits, when the ratio $\varepsilon = d/n$ is small or large, respectively. When ε is small, corresponding to small values of the external layer thickness, we can show by a simple rescaling of the Laplace equation, that to leading-order, and at relatively small values of the fraction S_{LS}, the profile is zero in the region $nS_{LS} < x < n$ and linearly varying with y in the region $0 < x < nS_{LS}$ (see also Figure 12, left panel). Thus, in this regime, the rate is to leading-order proportional to the saturation, a result with which our numerical solution in Figure 11 is qualitatively consistent. On the other hand, for large ε, namely, at large values of the external layer thickness, we can show using a similar approach that to leading-order, and at relatively large values of the fraction S_{LS}, the concentration at the surface is constant, and equal to 1, and hence the rate is constant, independent of the saturation S_{LS}, except for very small values of the latter (Figure 12, right panel). This finding is also qualitatively consistent with our numerical simulations for the much more complex model considered (and in which the external layer and the porous medium are coupled in a rather intricate way) (see Figure 11).

[39] Figure 13 shows the effect of the Peclet number on the concentration contours. For small values of Pe and ε, the profile is zero in the region $nS_{LS} < x < n$ and linearly varying with y in the region $0 < x < nS_{LS}$ (Figure 13, right panel). For larger values of Pe, the concentration contours become smoother in the x-direction and the concentration at the surface becomes constant (Figure 13, left panel), similar to the high ε case in the strictly diffusive process described above.

[40] Figure 11 shows a lack of a quantitative agreement between our 3-D pore-network coupled model and the *Suzuki and Maeda* [1968] results. We believe that this is due to the simplified coupling assumed in the latter model, where the no-flux condition $\partial\zeta/\partial y = 0$ is applied over the dry surface pores. This is not the case in the coupled case considered in this paper, where $\partial\zeta/\partial y$ is nonzero and flux is provided in "dry" pores. In fact, the effect of longer constant-rate periods over lower values of the surface liquid saturation is more pronounced in the actual case, namely, it will occur for lower values of ε, as the thickness of the dry region where diffusion takes place actually increases as the evaporating interface recedes deeper in the porous medium.

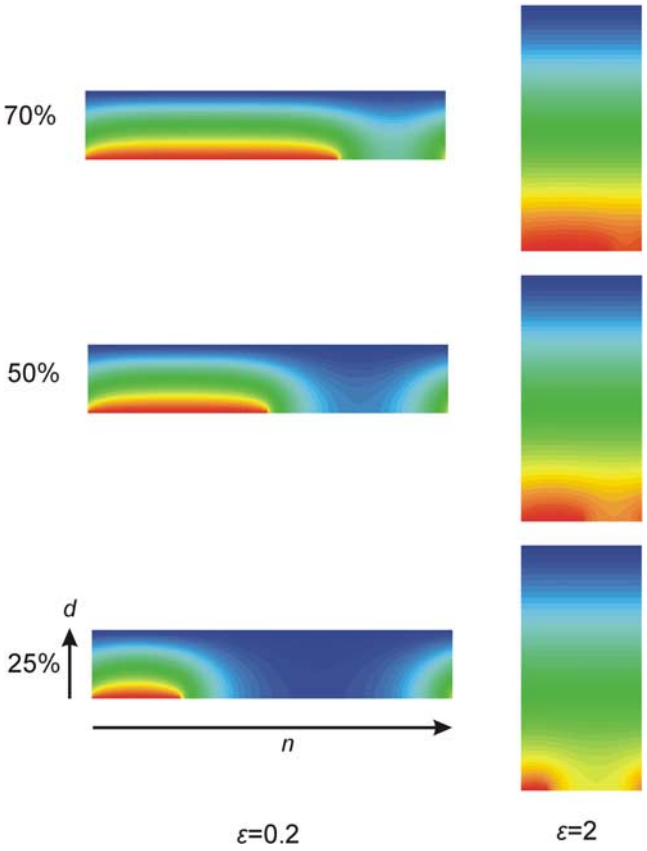

Figure 12. Concentration contours in the external mass boundary layer corresponding to the *Suzuki and Maeda* [1968] problem for the strictly diffusive case ($Pe = 0$) for two different values of the aspect ratio of the external layer and for three different values of the wet fraction of surface S_{LS}. The steady state diffusion equation is solved assuming constant concentration at the wet surface fraction S_{LS} and no-flux at the dry fraction $1\text{-}S_{LS}$. When ε is small (left panel), corresponding to small values of the external layer thickness d, the profile is approximately zero in the region $nS_{LS} < x < n$ and linearly varying with y in the region $0 < x < nS_{LS}$, particularly at lower values of S_{LS}. When ε is relatively large (right panel), namely, at large values of the external layer thickness d, the concentration at the surface is constant, and equal to 1, particularly at higher values of S_{LS}, and hence the rate is practically constant.

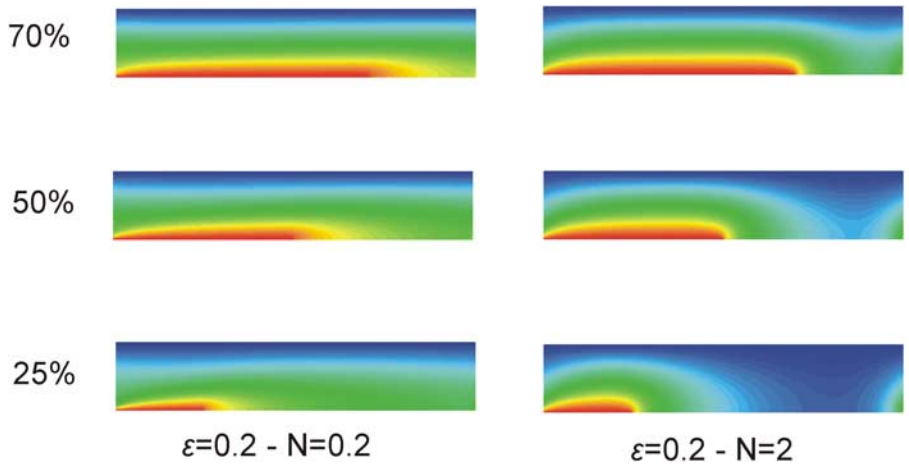

Figure 13. Effect of the Peclet number on the concentration contours over a discontinuous source of liquid for various values of the surface saturation [*Suzuki and Maeda*, 1968]. When $N = n/d^2Pe$ is small, namely, at large values of the external layer thickness d or large values of Pe, the concentration at the surface is constant, and equal to 1, and hence the rate is practically constant, independent of the saturation S_{LS}, except for very small values of the latter. Piston-like velocity profile.

Similar considerations apply when the Peclet number is not zero.

5. Conclusions

[41] In this paper we presented a pore-network model that couples convective-diffusive mass transfer over the external surface of a porous medium with mass transport mechanisms within the porous material; namely, the flow through liquid films that form at the pore walls and diffusion of the liquid vapors through the dry pores. The consideration of the external mass boundary layer offers a rigorous explanation of the constant-rate period.

[42] We have shown that the drying rate remains practically constant, as long as the liquid films span across the entire pore network and provide hydraulic connectivity between the bulk liquid front and the product surface. This condition is satisfied even for very low values of the surface saturation provided that the drying process is controlled by mass transfer over the porous medium surface, rather than mass transport within the porous material, namely, for large values of the boundary layer thickness and small values of the film-based capillary number. In this case the drying rate is inversely proportional to the mass boundary layer thickness d and independent of the capillary number Ca_F.

[43] The transition from the CRP to the FRP occurs when the liquid films that reach the product surface become so thin that they cannot sustain the mass transfer flux through the mass boundary layer over the product surface. During the FRP, drying is controlled by mass transport mechanisms within the porous material, namely, the flow through liquid films that form at the pore walls and diffusion through the dry pores. In this case the drying rate is inversely proportional to Ca_F for small values of Ca_F. Comparison with previous simpler models shows that a full, pore-network level model may be necessary to capture accurately all the relevant effects.

[44] It was also found that the effect of the Peclet number on the extent of the CRP is not major (under the simplifying assumption that the boundary layer thickness is not affected by its value) and the results are qualitatively similar to the diffusive case. The Peclet number affects the concentration contours. Higher values in the Peclet number lead to more uniform concentration profiles, as long as there are any films on the surface. As a result, the rate is kept constant for a longer period of time, and the critical saturation decreases. The effect is the same regardless of the particular velocity profile used. At much larger values of the ratio d/Ca_F, the extent of the CRP is larger, much like in the diffusive case. Therefore, for the fully developed case, and for a cell sufficiently downstream, the effect of the Peclet number is primarily through its effect on the boundary layer thickness d itself.

References

Bird, R. B., W. E. Stewart, and E. N. Lightfoot (1960), *Transport Phenomena*, John Wiley, Hoboken, N. J.

Blunt, M. J., M. Jackson, M. Piri, and P. H. Valvatne (2002), Detailed physics, predictive capabilities and macroscopic consequences for pore-network models of multiphase flow, *Adv. Water Resour.*, *25*(8–12), 1069–1089.

Chen, P., and D. C. T. Pei (1989), A mathematical model of drying processes, *Int. J. Heat Mass Transfer*, *32*(2), 297–310.

Dominguez, A., S. Bories, and M. Prat (2000), Gas cluster growth by solute diffusion in porous media: Experiments and automaton simulation on pore network, *Int. J. Multiphase Flow*, *26*, 1951–1979.

Dong, M., and I. Chatzis (1995), The imbibition and flow of a wetting liquid along the corners of a square capillary tube, *J. Colloid Interface Sci.*, *172*, 278–288.

Fatt, I. (1956), The network model of porous media, *Trans. Am. Inst. Min. Metall. Pet. Eng.*, *207*, 144–181.

Huinink, H. P., L. Pel, M. A. J. Michels, and M. Prat (2002), Drying processes in the presence of temperature gradients—Pore-scale modelling, *Eur. Phys. J. E*, *9*, 487–498, doi:10.1140/epje/i2002-10106-1.

Laurindo, J. B., and M. Prat (1996), Numerical and experimental network study of evaporation in capillary porous media: Phase distributions, *Chem. Eng. Sci.*, *51*(23), 5171–5185.

Laurindo, J. B., and M. Prat (1998), Numerical and experimental network study of evaporation in capillary porous media: Drying rates, *Chem. Eng. Sci.*, *53*(12), 2257–2269.

Leal, G. (1992), *Laminar Flow and Convective Transport Process*, Elsevier, New York.

Le Bray, Y., and M. Prat (1999), Three-dimensional pore network simulation of drying in capillary porous media, *Int. J. Heat Mass Transfer*, *42*, 4207–4224.

Li, X., and Y. C. Yortsos (1995), Theory of multiple bubble growth in porous media by solute diffusion, *Chem. Eng. Sci.*, *50*, 1247–1271.

Nowicki, S. C., H. T. Davis, and L. E. Scriven (1992), Microscopic determination of transport parameters in drying porous media, *Drying Technol.*, *10*(4), 925–946.

Prat, M. (1993), Percolation model of drying under isothermal conditions in porous media, *Int. J. Multiphase Flow*, *19*, 691–704.

Prat, M. (1995), Isothermal drying of non-hygroscopic capillary-porous materials as an invasion percolation process, *Int. J. Multiphase Flow*, *21*, 875–892.

Prat, M. (2007), On the influence of pore shape, contact angle and film flows on drying of capillary porous media, *Int. J. Heat Mass Transfer*, *50*(7–8), 1455–1468.

Prat, M., and F. Bouleux (1999), Drying of capillary porous media with a stabilized front in two dimensions, *Phys. Rev. E.*, *60*, 5647–5656, doi:10.1103/PhysRevE.60.5647.

Ransohoff, T. C., and C. J. Radke (1988), Laminar flow of a wetting liquid along the corners of a predominantly gas-occupied noncircular pore, *J. Colloid Interface Sci.*, *121*, 392–401.

Satik, C., and Y. C. Yortsos (1996), A pore-network study of bubble growth in porous media driven by heat transfer, *J. Heat Transfer*, *118*, 455–462.

Suzuki, M., and S. Maeda (1968), On the mechanism of drying of granular beds—Mass transfer from discontinuous source, *J. Chem. Eng. Jpn.*, *1*(1), 26–31.

van Brakel, J. (1980), Mass transfer in convective drying, in *Advances in Drying*, vol. 1, edited by A. S. Mujumdar, pp. 217–267, Taylor and Francis, Philadelphia, Pa.

Yiotis, A. G., A. K. Stubos, A. G. Boudouvis, and Y. C. Yortsos (2001), A 2-D pore-network model of the drying of single-component liquids in porous media, *Adv. Water Resour.*, *24*(3–4), 439–460.

Yiotis, A. G., A. G. Boudouvis, A. K. Stubos, I. N. Tsimpanogiannis, and Y. C. Yortsos (2003), Effect of liquid films on the isothermal drying of porous media, *Phys. Rev. E*, *68*(3), doi:10.1103/PhysRevE.68.037303.

Yiotis, A. G., A. G. Boudouvis, A. K. Stubos, I. N. Tsimpanogiannis, and Y. C. Yortsos (2004), Effect of liquid films on the drying of porous media, *AIChE J.*, *50*(11), 2721–2737.

Yiotis, A. G., I. N. Tsimpanogiannis, A. K. Stubos, and Y. C. Yortsos (2006), Pore-network study of the characteristic periods in the drying of porous media, *J. Colloid Interface Sci.*, *297*, 738–748, doi:10.1016/j.jcis.2005.11.043.

A. K. Stubos and A. G. Yiotis, National Center for Scientific Research "Demokritos," Aghia Paraskevi 15310, Greece. (yiotis@ipta.demokritos.gr)

I. N. Tsimpanogiannis, Earth and Environmental Sciences Division (EES-6), Los Alamos National Laboratory, Los Alamos, NM 87545, USA.

Y. C. Yortsos, Department of Chemical Engineering, University of Southern California, Los Angeles, CA 90089, USA.